



HAL
open science

Fish scale of *Sardina pilchardus* as a biosorbent for the removal of Ponceau S dye from water: Experimental, designing and Monte Carlo investigations

A. Jaafar, A. Darchen, A. Driouich, Z. Lakbaibi, A. Boussaoud, B. Chatib, Y. Laftani, M. El Makhfouk, M. Hachkar

► To cite this version:

A. Jaafar, A. Darchen, A. Driouich, Z. Lakbaibi, A. Boussaoud, et al.. Fish scale of *Sardina pilchardus* as a biosorbent for the removal of Ponceau S dye from water: Experimental, designing and Monte Carlo investigations. *Inorganic Chemistry Communications*, 2022, 137, pp.109196. 10.1016/j.inoche.2022.109196 . hal-03596332

HAL Id: hal-03596332

<https://hal.science/hal-03596332>

Submitted on 30 Mar 2022

HAL is a multi-disciplinary open access archive for the deposit and dissemination of scientific research documents, whether they are published or not. The documents may come from teaching and research institutions in France or abroad, or from public or private research centers.

L'archive ouverte pluridisciplinaire **HAL**, est destinée au dépôt et à la diffusion de documents scientifiques de niveau recherche, publiés ou non, émanant des établissements d'enseignement et de recherche français ou étrangers, des laboratoires publics ou privés.



Distributed under a Creative Commons Attribution - NonCommercial 4.0 International License

Fish scale of *Sardina pilchardus* as a biosorbent for the removal of Ponceau S dye from water: Experimental, designing and Monte Carlo investigations

Adil Jaafar^{1,*}, André Darchen², Anas Driouich³, Zouhair Lakbaibi⁴, Abdelghani Boussaoud⁵, Baylassane Chatib⁵, Yasmine Laftani⁵, Mohammed El Makhfouk⁵, Mohsine Hachkar⁵

¹*Ecole Supérieure de l'Éducation et de la Formation de Berrechid, Hassan Ist University Settat, Morocco*

²*UMR CNRS n°6226 - Institut des Sciences Chimiques de Rennes, ENSCR, 11 Allée de Beaulieu – CS 50837 – 35708 Rennes Cedex 7, France*

³*Laboratory of Chemical Engineering and Environment, Faculty of Sciences and Techniques, Hassan II University, Mohammedia, Morocco*

⁴*Laboratory of Molecular Chemistry, Materials and Environment, Multidisciplinary Faculty - Nador, Mohamed First University, Oujda, Morocco*

⁵*Higher School of Technology, Cadi Ayyad University, Safi, Morocco*

* Corresponding author:

E-mail address: jaafarfstgm@gmail.com; Mobile: +2120660202754 (Adil Jaafar)

Abstract

In this work, the removal of the hazardous Ponceau S dye (PS) from aqueous solutions was investigated using Fish Scale (FS) of *Sardina pilchardus* as low-cost adsorbent. Different relevant factors such as contact time, initial pH, initial PS concentration, biosorbent dose and temperature were examined to evaluate their effects. The optimization of these factors was performed with a Central Composite Design (CCD). Optimized parameters (pH = 2.1, [PS] = 35 mg L⁻¹, m(FS) = 250.0 mg, V = 200 mL and T = 303 K) were found with the maximum of 96.58% PS loading onto FS. The kinetics results show that the pseudo-first-order model gave a better fit than the pseudo-second-order model. Freundlich isotherm gave a better fit than Langmuir model. The thermodynamic factors, such as Gibb's free energy change (ΔG), enthalpy change (ΔH) and entropy change (ΔS) have been calculated. The biosorption was found to be a spontaneous and endothermic process. The desorption of PS from exhausted biosorbent was investigated in alkaline solution. Furthermore, Monte Carlo (MC) and radial distribution function (RDF) simulations were achieved to obtain a better understanding of biosorption mechanism of PS on both collagen and hydroxyapatite (HDA) which are the main constituents of FS. The results showed that PS presented a better biosorption on collagen than on the HDA surface. The biosorption of PS onto studied surfaces was spontaneous, characterized highly by chemical interactions and slightly by physical ones. Since FS is a low-cost marine waste, it presents interesting perspectives in the treatment of contaminated wastewaters on a large-scale.

Keywords: Biosorption; Marine waste; Kinetics; Thermodynamic parameters; Optimization; Radial distribution function

1. Introduction

One of the most recent challenges facing environment is to sustain and conserve water resources (groundwaters and surface waters). The importance of these challenges increases with the development of urban, agricultural, and industrial activities that generate a large amount of wastewater. Textile industries are known as the main contributors of water contamination because they consume large volumes of water through different processes [1]. Wastewaters extensively vary in terms of composition due to the impurity in fibers and the chemical compounds arising from the involved steps. Major problems in wastewaters from textile industries concern dyes. The annual production of dye is more than 7000 metric tons [2], in which 2% are lost in aqueous effluents and about 10 % are discharged during the coloration process [3]. The release of the dyes causes many environmental problems into water where they are the more visible pollutants. Because of their chemical structure, dyes might cause potentially dangerous bioaccumulation and ecotoxicity. The treatment of increasing number of pollutants in wastewater needs the research of new biosorbents. In the present paper Ponceau S (PS) was used as a model of dye and its removal was investigated by biosorption onto Fisch Scale (FS).

Acid Red 112 or PS, is an anionic diazo dye which is found in several applications of food process and in biochemistry. It is also used in clinical laboratories [4] and in dying industry of textile and leather [5]. PS is known as a toxic and carcinogen chemical [4,6]. Its removal has been investigated by numerous researchers. Photocatalytic degradations of PS were performed in the presence of various photocatalysts such as Nb_2O_5 with commercial activated carbon [7], methylene blue immobilized in resin Dowex-11 [5,8], nanosized PbO [9], ZnO [10-12] and nano structured Ni-doped TiO_2 thin film [13]. Mineralization of PS was carried out in the presence of strong oxidants under photochemical activation [14-15], Fenton process [16], and Fenton-like processes [17,18]. Despite its easiness to use, adsorption or biosorption methods were rarely applied to PS removal. Efficient processes were observed with nanofibrous membrane [19], chitin [20], nanoparticles of MgO [6] and AlPO_4 and surface modified AlPO_4 [21,22].

FS are found in marine wastes, and they are able to work as low-cost biosorbents. They have been already used in wastewater treatments, mainly for the removal of heavy metals, dyes and pharmaceutical [23-26]. To our knowledge, FS of *Sardina pilchardus* have never been applied to the treatment of PS. Besides, a computational study was

developed in order to investigate the biosorption behavior of collagen and HAD during this process.

In the present research work, the biosorption of PS into FS was investigated. The effect of various process factors was studied, including their interactions by using a Central Composite Design (CCD) according to the response surface methodology (RSM). Applying CCD, it is possible to evaluate the interactions of factors on biosorption efficiency and to determine the optimum operational conditions for the process with a small number of experiments [27]. The isothermal study was analyzed using Freundlich and Langmuir isotherm models. The pseudo-second-order and pseudo-first-order models were also applied to characterize the kinetic process. Thermodynamic study was also applied to complete the investigation of PS removal by biosorption onto FS. Since regeneration and reusability of adsorbents are important steps in the research of an economical process [28-30], the regeneration of the exhausted biosorbent FS was studied. MC and RDF calculations were used to investigate the biosorption behavior of PS onto both collagen and HDA which are the main constituents of FS. This computational study provided highlights for a better knowledge of the biosorption process of PS dye on FS surfaces. All the results indicated that FS was efficient in the removal of PS.

2. Experimental section

2.1. Reagents

PS was purchased from Reactifs Ral. The chemical structure and some properties of the PS are given in Fig. 1 and Table 1, respectively. The other chemicals, sodium chloride (NaCl), sodium hydroxide (NaOH) and hydrochloride acid (HCl) were purchased from Scharlau Chemie. The collection and preparation of the biosorbent FS of *Sardina pilchardus* are described in a precedent paper [31].

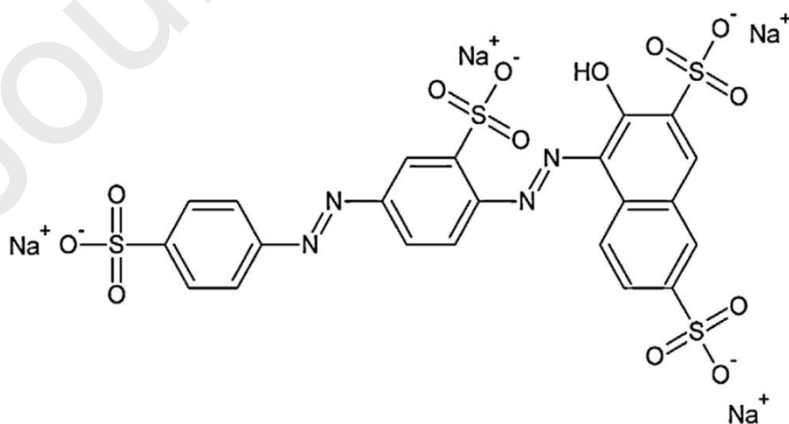


Fig. 1. Chemical structure of PS

Table 1. Some properties of PS dye

IUPAC name	3-Hydroxy-4-(2-sulfo-4-[4-sulphophenylazo]phenylazo)-2,7-naphthalenedisulphonic acid sodium salt
Synonym	Acid Red 112
C. I. Number	27195
Type	Anionic
Molecular weight	760.57g mol ⁻¹
Azo group number	2
λ_{\max}	520nm
Molecular formula	C ₂₂ H ₁₂ N ₄ O ₁₃ S ₄ Na ₄

2.2. Biosorption studies

Biosorption experiments were conducted by adding 250 mg of FS to a set of 500 mL conical flasks containing 200 mL of PS solutions with initial concentrations of 35 mg L⁻¹ at pH 2.1 and T = 296 K. The flasks were shaken at a constant agitation speed, with contact time of 60 min. The effect of biosorbent mass was studied by performing series of experiments at a biosorbent mass ranging from 50 mg to 300 mg.

In order to examine the effect of initial PS concentration and solution pH, 250 mg of biosorbent were used at T = 296 K. These experiments were carried out by changing the initial PS concentration from 10 mg L⁻¹ to 45 mg L⁻¹, the pH from 2.10 to 11.20. The initial pH was adjusted by adding solutions of 0.1 M HCl or 0.1 M NaOH. Each experiment was replicated three times.

After a centrifugation at 3000 rpm for 5 min, the PS concentration was measured by UV–visible spectrophotometry (Rayleigh UV-1800) at maximum wavelength, $\lambda_{\max} = 520$ nm. The removal of PS was calculated by Eq. (1) where $[PS]_t$ is the PS concentration at reaction time and $[PS]_0$ is the PS initial concentration.

$$\text{Percentage removal (\%)} = \left(1 - \frac{[PS]_t}{[PS]_0}\right) \times 100 \quad (1)$$

The adsorbed quantity q_t (mg g⁻¹) was calculated from the concentration of PS with Eq. (2) where C_0 (mg L⁻¹) and C_t (mg L⁻¹) are PS initial concentration and PS concentration at time t , respectively, V is the volume of the dye solution (L) and m is the mass of FS (g).

$$q_t = (C_0 - C_t) \frac{V}{m} \quad (2)$$

The regeneration of the biosorbent was studied by placing 250 mg of FS into 200 mL of dye solutions, with initial concentrations of 35 mg L⁻¹ at pH 2.1 and T = 23°C.

Then, the dye-loaded FS were separated from the solution by a centrifugation and dried in an oven at 60°C for 2 h. Finally, the dye-loaded FS were agitated with 200 mL of deionized distilled water at pH 10.70 and 23°C for 2 h.

The point of zero charge (pH_{pzc}) was determined by the salt addition method [32,33]. The initial pH_i of 200 mL of 0.01 M NaCl solution was adjusted to a pH in the range 2–12. Then, 250 mg of FS were added to each solution. The solutions were shaken for 24 h at 23°C, and the final pH of the solutions (pH_f) was determined. The point of zero charge (pH_{pzc}) is the point where the curve pH_f vs. pH_i intersects the line $pH_f = pH_i$.

The X-Ray Diffraction (XRD) analysis was investigated by using a Rigaku diffractometer. The XRD patterns were obtained by using the Cu K α radiation (1.5418 Å), a voltage of 40 kV, 40 mA of current, a step size of 0.02°, a step time of 1 s and 2θ in the range 10° - 60°.

2.3. Kinetic study

The pseudo-first-order kinetic has been investigated with Eq. (3) [34] where q_e (mg g⁻¹) and q_t (mg g⁻¹) are the sorption capacities at equilibrium and at time t , respectively, k_1 (min⁻¹) is the rate constant of the pseudo-first-order sorption and t is the time.

$$\ln(q_e - q_t) = \ln(q_e) - k_1 t \quad (3)$$

The pseudo-second-order kinetic equation is given by Eq. (4) [35] where q_e (mg g⁻¹) and q_t (mg g⁻¹) are the sorption capacities at equilibrium and at time t , respectively, t is the time and k_2 is the rate constant (g mg⁻¹ min⁻¹).

$$\frac{t}{q_t} = \frac{1}{k_2 q_e^2} + \frac{1}{q_e} t \quad (4)$$

Besides the value of R², the validity of each model was determined by the sum of error squares (SSE) given by Eq. (5):

$$SSE = \sum_{i=1}^n (y_{exp} - y_{cal})^2 \quad (5)$$

Where y_{exp} is the experimental value and y_{cal} is the calculated value.

2.4. Biosorption isotherm models

Biosorption isotherms represent an important step to know how molecules or ions of adsorbate interact with the biosorbent surface at the equilibrium conditions. The isotherms constants are critical in optimizing the usage of biosorbents. Many isotherm models have been reported and used to describe the biosorption of mono solute which

could be classified into various classes. In this paper, Langmuir [36] and Freundlich [37] isotherms were employed to investigate the biosorption behavior.

The main hypotheses of the Langmuir biosorption isotherm are: (i) the biosorption is mainly due to a saturated monolayer of adsorbate molecules on the biosorbent surface, (ii) the energy of biosorption is constant, and (iii) in the plane of the biosorbent surface, there is no transmigration of adsorbed dye molecules. Langmuir isotherm is identified by Eq. (6) [36] where C_e and q_e are adsorbate concentration (mg L^{-1}) and adsorbed quantity (mg g^{-1}) at equilibrium, respectively.

$$\frac{C_e}{q_e} = \frac{1}{q_m} C_e + \frac{1}{q_m K_L} \quad (6)$$

The plot of $1/q_e$ versus $1/C_e$ should give a straight line. The slope has the value of $1/K_L q_m$, where K_L (L mg^{-1}) is the Langmuir constant and q_m (mg g^{-1}) is the maximum biosorption capacity [38]. According to the Langmuir constant K_L (L mg^{-1}) and the highest initial PS concentration C_o (mg L^{-1}), the dimensionless equilibrium parameter R_L is given by Eq. (7) [39].

$$R_L = \frac{1}{1 + K_L C_o} \quad (7)$$

R_L value characterizes the nature of the biosorption process. For R_L values (>1), ($=1$), ($0 < R_L < 1$) and ($=0$), the process is unfavorable, linear, favorable and irreversible, respectively [40].

Freundlich model [37] considers a mono-layer adsorption of solute and suggests that the adsorbent has surface supporting sites of various affinities or a heterogeneous surface, and the existence of an interaction between the adsorbed molecules onto that heterogeneous surface [37]. The Freundlich equation assumes that the biosorption energy exponentially decreases on completion of the active centers of a biosorbent. The Freundlich biosorption isotherm is given by Eq. (8) [41] where C_e (mg L^{-1}) is the adsorbate dose at equilibrium and q_e (mg g^{-1}) is the adsorbed quantity.

$$q_e = K_F C_e^{\frac{1}{n}} \quad (8)$$

Freundlich constants (K_F) and (n) characterize the adsorption capacity and the intensity of the adsorption and influence the adsorption process. These constants were found by drawing a straight-line $\ln(C_e)$ versus $\ln(q_e)$ which gave as intercept $\ln(K_F)$ and a slope of $1/n$. The n value is a measure of strength and the nature of the adsorption process and of the distribution of active sites. The intensity of adsorption less than one ($n < 1$) corresponds to an adsorption process of chemical nature. Favorable adsorption conditions are characterized by an adsorption intensity greater than one ($n > 1$) [42].

2.5. Central Composite Design

The CCD was used to determine the regression model equations, operating parameters and to optimize the biosorption process from the appropriate experiments. It was also a good tool to find the optimum process of various parameters. Moreover, it was useful in studying the interactions of the parameters affecting the process.

To make a well prediction and to have a descriptive quality in the whole experimental domain, by minimizing the experiment number, the design of the plan required 31 experiments with Eq. (9) where k was the number of independent variables and N_0 was the number of repetitions of the central points. Table 2 gathers the levels attributed to each variable.

$$2^k + 2k + N_0 = 16 + 8 + 7 = 31 \quad (9)$$

Table 2. Parameters, experimental range and level of independent variables

Natural variables (x_i)	Units	Coded variables X_1, X_2, X_3, X_4^*					Δx
		$-\alpha$	-1	0	1	$+\alpha$	
$x_1 = \text{pH}$	-	2.10	2.35	2.60	2.85	3.10	0.25
$x_2 = [\text{PS}]$	(mg /L)	15	25	35	45	55	10
$x_3 = \mathbf{m}_{(\text{FS})}$	(mg)	50	120	190	260	330	70
$X_4 = \text{T}$	(K)	293	298	303	308	313	5

$$*\alpha = 2.00, X_i = \frac{x_i - x_0}{\Delta x_i}$$

Data were investigated by the analysis of variance method. Also, according to the alpha risk, a statistical analysis of the probability value was carried out to compare experimental and theoretical values F (Fisher-Snedecor table). The optimal values of the operation parameters were given by response surface plots [27,43].

Table 3 shows the 31 experiments. The experimental conditions of the i^{th} experiment are defined by the i^{th} line of this matrix [43]. In order to minimize the error due to the experiments, the plan was carried out with a randomized order. The results are grouped in Table 3. The interpretation of the results was obtained by the analysis of variance of the model, the computation of the estimates of the coefficients for the factors and their interactions, and the determination of their significance were based on specific statistical tests [44].

Table 3. The experimental data for responses according to central composite design

Run		Coded variables values			Uncoded variables values				Efficiency	
Logical	Random	X_1	X_2	X_3	X_3	x_1	x_2	x_3	x_4	(%)

		pH	[PS]	m (FS)	T	pH	[PS]	m (FS)	T	
1	26	-1	-1	-1	-1	2.35	25	120	298	90.75
2	24	-1	-1	-1	1	2.35	25	120	308	89.4
3	31	-1	-1	1	-1	2.35	25	260	298	93.87
4	18	-1	-1	1	1	2.35	25	260	308	95.61
5	13	-1	1	-1	-1	2.35	45	120	298	63.76
6	30	-1	1	-1	1	2.35	45	120	308	85.21
7	2	-1	1	1	-1	2.35	45	260	298	96.58
8	19	-1	1	1	1	2.35	45	260	308	89.26
9	16	1	-1	-1	-1	2.85	25	120	298	50.49
10	23	1	-1	-1	1	2.85	25	120	308	47.51
11	21	1	-1	1	-1	2.85	25	260	298	53.61
12	3	1	-1	1	1	2.85	25	260	308	36.2
13	27	1	1	-1	-1	2.85	45	120	298	34.9
14	6	1	1	-1	1	2.85	45	120	308	33.56
15	1	1	1	1	-1	2.85	45	260	298	42.39
16	28	1	1	1	1	2.85	45	260	308	34.99
17	11	-2	0	0	0	2.1	35	190	303	90.02
18	5	2	0	0	0	3.1	35	190	303	20.35
19	7	0	-2	0	0	2.6	15	190	303	85.28
20	29	0	2	0	0	2.6	55	190	303	64
21	25	0	0	-2	0	2.6	35	50	303	68.54
22	17	0	0	2	0	2.6	35	330	303	76.27
23	22	0	0	0	-2	2.6	35	190	293	73.24
24	20	0	0	0	2	2.6	35	190	313	69.42
25	4	0	0	0	0	2.6	35	190	303	82.73
26	8	0	0	0	0	2.6	35	190	303	81.98
27	9	0	0	0	0	2.6	35	190	303	82.04
28	10	0	0	0	0	2.6	35	190	303	83.05
29	12	0	0	0	0	2.6	35	190	303	82.25
30	14	0	0	0	0	2.6	35	190	303	81.49
31	15	0	0	0	0	2.6	35	190	303	83.03

2.6. Simulation software

Biosorption of PS onto collagen and HDA as periodic surfaces in acidic medium (100H₂O, 50H₃O⁺ and 50Cl⁻) was explored by Monte Carlo and RDF simulations using

forcite code calculations combined to the COMPASS II force-field using Material studio software package [45].

3. Results and discussion

3.1. Characterization of FS biosorbent

The FS structure was characterized in a precedent paper by Scanning Electron Microscopy (SEM), Energy Dispersion Spectroscopy, X-Ray Diffraction (XRD) and Fourier Transform Infra-Red (FT-IR) spectroscopy [44]. The non-mineralized organic component (type I collagen) and the mineralized inorganic component hydroxyapatite $\text{Ca}_{10}(\text{PO}_4)_6(\text{OH})_2$ are the main constituents of FS [46-49]. Furthermore, Fig. 2 shows the XRD diagram of FS. The great width of reflections shows that FS contained nano-crystallites of hydroxyapatite. Their sizes can be obtained thanks to the Scherrer equation (Eq. (10)) where D (nm) is the size of the crystallite, λ is the wavelength of Cu $K\alpha$ ($\lambda=0.15418$ nm), β (rad) is the full width at half maximum, and θ is the diffraction angle [49]. The isolated reflection at 2θ of 26.5° , corresponding to the (002) Miller plan, was chosen for the calculation leading to the crystallite size of 10.5 ± 1 nm. This result agrees with the size measured at 12 nm for fish scale of *Catla catla* after calcination at 200°C [50] or with the size of 20-30 nm which was measured by SEM with transmission mode for hydroxyapatite particles of *tilapia* fish scales [51].

$$D = \frac{0.89 \lambda}{\beta \cos(\theta)} \quad (10)$$

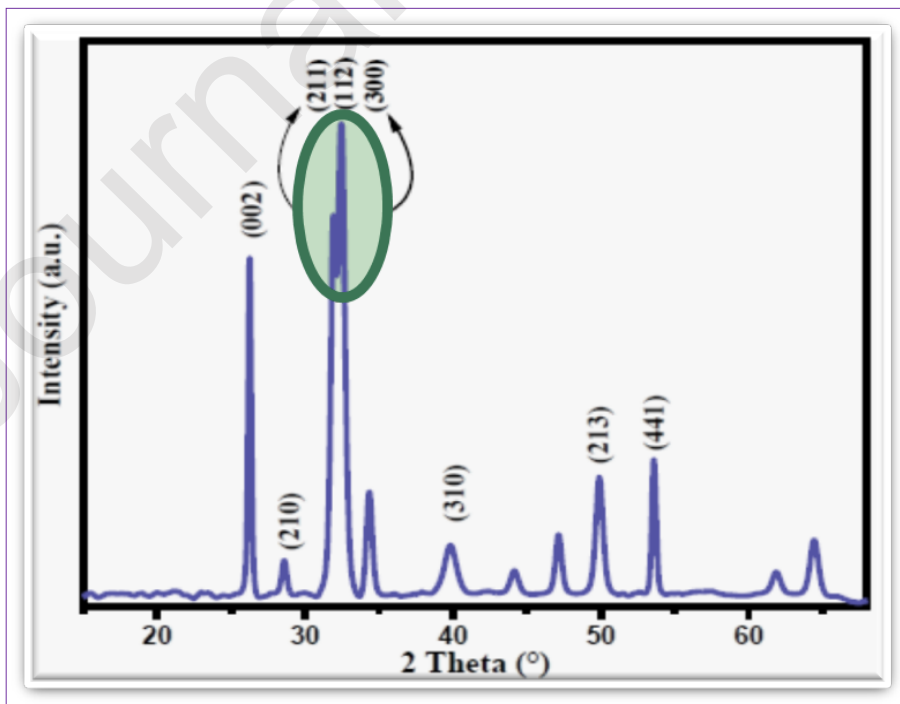


Fig. 2. XRD pattern of FS

3.2. Initial pH effect

pH_{pzc} characterize the change in the biosorbent surface. It corresponds to a net surface charge of zero, and it gives information about the electrostatic interaction between biosorbent and adsorbate. As shown in Fig. 3, the pH_{pzc} value of 8.5 was obtained for FS

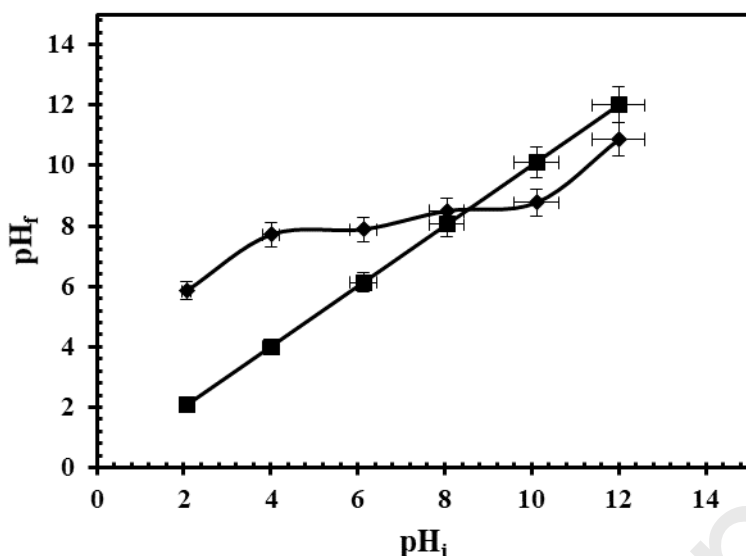


Fig. 3. Determination of point zero charge (pH_{pzc}) of FS

Fig. 4 presents the pH effect on biosorption behavior of PS onto FS at pH 2.10–11.20. The greatest removal was observed at pH 2.10. In aqueous solution, PS dissolves and leads to their corresponding dye ions $\text{D}(\text{SO}_3^-)_4$ and Na^+ . The FS surface is positively charged when the pH is lower than 8.5. Therefore, the biosorption occurs between the dissociated dye ions ($\text{D}(\text{SO}_3^-)_4$) and FS surface sites. When the pH increased from 2.70 to 11.20, the uptake decreased from its greatest value of 34.26 mg g^{-1} to 0.59 mg g^{-1} . This was the result of a decrease in electrostatic interactions between the dye anion and FS. Such mechanism proves the cause of the observed biosorption under strongly acidic conditions. The optimum pH for biosorption was found to be 2.10 for the following studies. These results demonstrates that the electrostatic interactions were the main factor of PS dye biosorption onto FS surface.

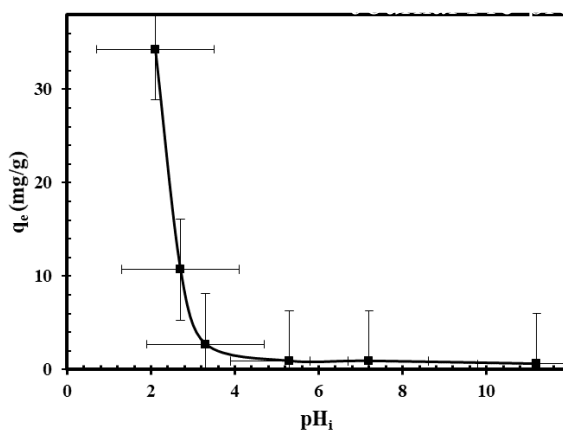


Fig. 4. Effect of pH on the PS biosorption onto FS ($[PS]_0 = 35 \text{ mg L}^{-1}$, $m(\text{FS}) = 250 \text{ mg}$, $V = 200 \text{ mL}$, contact time = 60 min, $T = 296 \text{ K}$)

3.3. Effect of contact time

This effect was studied by varying the agitation time using aqueous solution containing various concentrations of PS. Fig. 5 shows that the removal efficiency increases with the duration of agitation time, reaching nearly maximum removal at contact time of 60 min. Thereafter, the adsorbed quantity becomes nearly constant. The reason may be due to the fact that, initially all the biosorbent sites were free and the PS concentration was high. Afterwards, the PS biosorption capacity of FS decreased significantly due to the decrease in available biosorption sites as well as PS concentration.

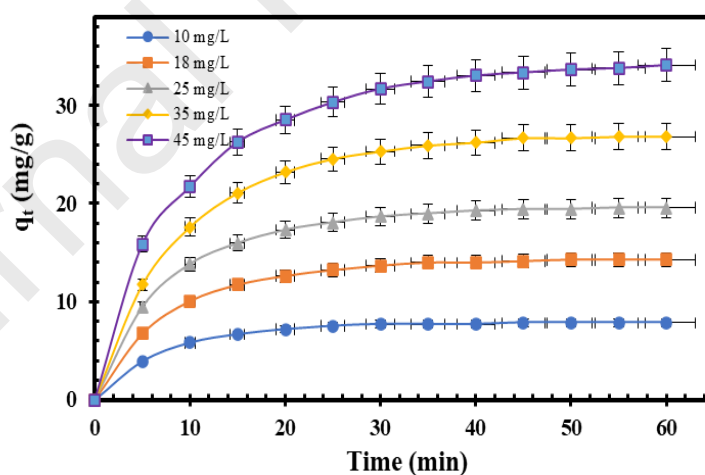


Fig. 5. Effect of contact time and PS dose on its biosorption into FS ($m(\text{FS}) = 250 \text{ mg}$, $\text{pH} = 2.10$, $V = 200 \text{ mL}$, $T = 296 \text{ K}$)

3.4. Effect of PS dose

This effect of PS on its removal was studied at room temperature. Fig. 5 presents the influence of the PS dose on its biosorption. It is evident that the biosorption of PS rapidly occurs during the first 10 min, then gradually it reaches a maximum value corresponding

to an equilibrium at around 60 min. Many vacant surface sites would be available for biosorption during the initial stage of the treatment, and after a few times, the remaining vacant surface sites would be difficult to be occupied due to repulsive forces between adsorbed PS and free PS in solution.

3.5. FS dose influence

This influence on PS biosorption is presented in Fig. 6. Results show that the biosorption efficiency of FS increased when FS dose increased. After 60 min of stirring the mixture of the dye and FS, the biosorption efficiency varied from 33.76% for 50 mg of FS to 96.58% for 300 mg of FS. The improved removal percentage of PS may be explained by the increase of FS dose and the concomitant increase of the available surface for adsorption [52,53]. The best dose of biosorbent was found to be 1.25 g L⁻¹ of FS for the following studies. This quantity gave the same removal percentage than 1.5 g L⁻¹ (96.58%).

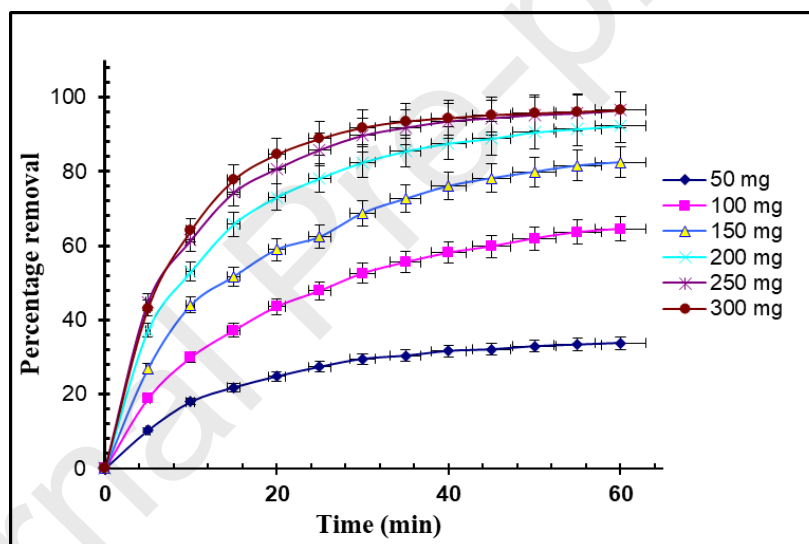


Fig. 6. Effect of FS dose on the biosorption of PS ($[PS]_0 = 35 \text{ mg L}^{-1}$, $\text{pH} = 2.10$, $V = 200 \text{ mL}$, $T = 296 \text{ K}$)

3.6. Kinetic study

The kinetic parameters are gathered in Table 4. Both kinetic models give a good correlation coefficient R^2 . For the pseudo-second-order a large gap is observed between the calculated q_{cal} and the experimental q_{exp} quantities. So, the biosorption of PS onto FS does not follow this model. For the Lagergren pseudo-first-order there is a good agreement between the calculated q_{cal} and the experimental q_{exp} quantities. In addition, the value of SSE of the pseudo-first-order model was lower than that the one of the

pseudo-second-order model. These results show that the pseudo-first-order model provides a better fit for the experimental data.

Table 4. Kinetic parameters for the biosorption of PS onto FS

Kinetic models	Parameters	Value
Pseudo-first-order	k_1 (min ⁻¹)	0.0783
	q_{exp} (mg g ⁻¹)	34.11
	q_{cal} (mg g ⁻¹)	32.97
	R^2	0.99
	SSE	0.001
Pseudo-second-order	k_2 (g mg ⁻¹ min ⁻¹)	0.003
	q_{cal} (mg g ⁻¹)	38.31
	R^2	0.99
	SSE	0.04

3.7. Isothermal study of the biosorption

Table 5 summarizes Freundlich and Langmuir isotherm data for the PS biosorption. The R^2 value of the Langmuir model was lower than that the one of the Freundlich model, showing that the Freundlich isotherm model gives a better fit of the experimental data than the Langmuir isotherm model. Therefore, the Freundlich model was the most appropriate isotherm to describe the equilibrium data for PS biosorption. In contrast, the Freundlich constant n value ($n = 5.55$) for the biosorption of PS onto FS shows that the biosorption is favorable.

Table 5. Isotherm parameters for the biosorption of PS onto FS

Isotherm models	Parameter	Value
Langmuir	K_L (L mg ⁻¹)	1.28
	q_m (mg g ⁻¹)	56.50
	R^2	0.91
	R_L	0.017
Freundlich	K_F (mg g ⁻¹)	0.03
	n	5.55
	R^2	0.99

3.8. Temperature effect and thermodynamic parameters

Fig. 7 presents the temperature effect on the biosorption of PS by FS. The results show that the biosorption of PS by FS decreased from 97.90 % to 83.26 % with an increase in temperature from 298 K to 328 K. The quantity of PS adsorbed by FS decreased when the temperature increased, suggesting that a lower temperature favored the PS removal from the aqueous solution. This tendency might be due to a decrease of the number of active sites which are involved in the biosorption when the temperature increased. Table 6 shows that the K_L values increased with the temperature. This observation means that the PS biosorption phenomenon on FS is governed by an endothermic process [54].

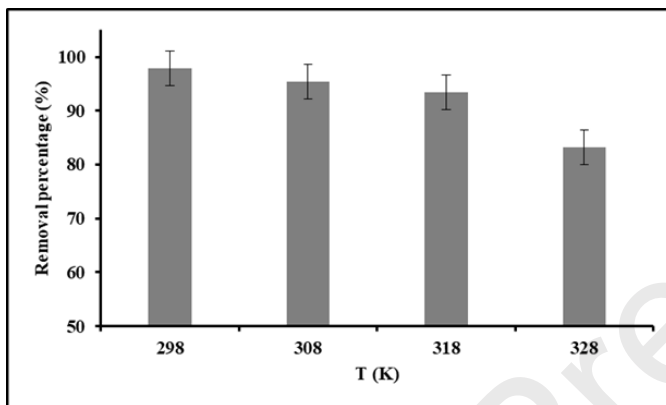


Fig. 7. Effect of temperature on biosorption of PS onto FS ($[PS]_0 = 45 \text{ mg L}^{-1}$, $m(\text{FS}) = 250 \text{ mg}$, $\text{pH} = 2.10$ and $V = 200 \text{ mL}$)

The thermodynamic parameters, such as Gibb's free energy change (ΔG), enthalpy change (ΔH), entropy change (ΔS), are the main parameters which determine the mechanism of a biosorption process. The temperatures used in the thermodynamic study were 298 K, 308 K, 318 K and 328 K. The thermodynamic parameters were calculated by using Eqs. (11-13) [54,55]. The thermodynamic equilibrium constant (K_C ; dimensionless) was calculated from the Langmuir constant (K_L) [55]. When the K_L unit is expressed in L mg^{-1} , Zhou and Zhou [56] recommended that K_C can be obtained as a dimensionless constant by multiplying K_L by the molecular weight of adsorbate M_w , 1000, and then 55.5 (Eq. (12)).

$$\Delta G = -RT \ln(K_C) \quad (11)$$

$$K_C = K_L \times M_w \times 1000 \times 55.5 \quad (12)$$

$$\ln(K_C) = \frac{\Delta S}{R} - \frac{\Delta H}{RT} \quad (13)$$

The thermodynamic parameters were obtained with the following units: ΔG (J mol^{-1}); ΔS ($\text{J mol}^{-1} \text{ K}^{-1}$); ΔH (J mol^{-1}). R ($8.314 \text{ J mol}^{-1} \text{ K}^{-1}$) is the universal gas constant, T (K) is the

absolute solution temperature, K_L ($L \cdot mg^{-1}$) is the Langmuir constant, M_w ($g \cdot mol^{-1}$) is the molecular weight of adsorbate (PS), the 1000 factor changes the mass unit of g to mg, and the factor 55.5 is the mole number of H_2O in 1 L.

Values of $\ln(K_C)$ are given in Table 6. From Eq. (13), a plot of $\ln(K_C)$ versus $1/T$ produces a straight line with a slope of $\Delta H/R$ and an intercept of $\Delta S/R$, which can be used to calculate the values of thermodynamic parameters. The results are given in Fig. 8 and Table 6. The positive value of ΔH confirmed that the biosorption process was endothermic which adsorbed energy in the form of heat from its surroundings. This is due to the fact that the PS dye must displace more than one water molecule for their biosorption, which causes the endothermicity of the biosorption process [57]. Meanwhile, the negative values of Gibb's free energy change (ΔG) at all temperatures suggested that the biosorption of PS onto FS was thermodynamically favorable and spontaneous. The decreased negative values of ΔG , along with the increasing temperatures, confirmed that the accumulation phenomenon of PS dye onto PS was more feasible at a lower temperature [54]. Lastly, the positive value of entropy change (ΔS) showed an increase in random motion of the PS molecules at the solid/solution interface during the biosorption process. The positive ΔS value also confirms that the biosorption phenomenon involves a dissociative mechanism [54]. Moreover, the positive value of ΔS also involves the increased degree of freedom of PS dye in the solution.

In addition, it is well known that physisorption, such as van der Waals interactions, has usually ΔG values lower than -20 kJ mol^{-1} , and electrostatic interaction ranges from -20 to -80 kJ mol^{-1} . Chemisorption band strengths can be found in the range from -80 to -400 kJ mol^{-1} [58,59]. Referring to the results in Table 6, and even at different temperatures, considering the values of ΔG , the biosorption of PS by FS confirms that the process is a physisorption one.

Table 6. Thermodynamic parameters calculated from the Langmuir constant

T (K)	Van't Hoff equation	K_L ($L \cdot mg^{-1}$)	$\ln(K_C)$	ΔG ($kJ \cdot mol^{-1}$)	ΔH ($kJ \cdot mol^{-1}$)	ΔS ($J \cdot mol^{-1}$)
298		1.23	17.73	-43.93		
308	$y = -1467.6x + 22.652$	1.46	17.86	-45.75	12.20	188.33
318	$R^2=0.991$	1.77	18.06	-47.74		
328		1.98	18.17	-49.55		

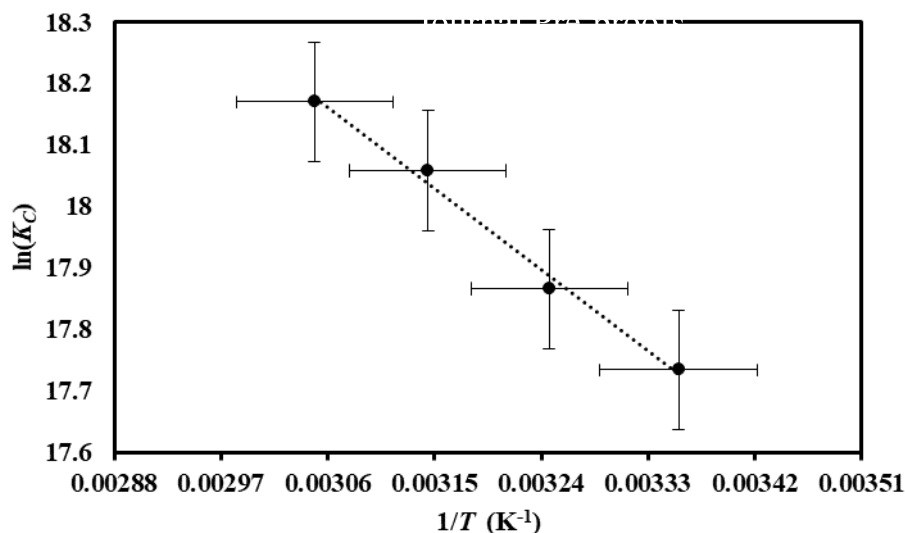


Fig. 8. Plot of $\ln(K_C)$ versus $1/T$ for the determination of the thermodynamic parameters

3.9. Desorption study

To make the process more economical, desorption (the reverse process of biosorption) was studied. The basis of biosorption interactions was electrostatic, so during desorption process, electrostatic interaction should be eliminated as observed by Tarhan *et al* [28]. The dye on the surface of FS was quantitatively desorbed by breaking their electrostatic interaction bonds at pH 10.70.

3.10. Optimization using CCD

3.10.1. Analysis of variance

This analysis was done to see the effect of the selected parameters on the response [41]. As shown in Table 7, the $F_{statistic}$ value of regression (40.6887), for the PS biosorption efficiency, is higher than $F_{th}(F_{0.01}(14.16) = 5.27)$. The largest F -value indicates that the response variation can be explained by the regression equation.

The p -value confirms the interpretation demonstrated by Fisher test. The associated p -value of the regressions is lower than 0.05. Therefore, this result means that there is no statistical difference between the predicted and experimental values of the models.

Table 7. Variance analysis for PS biosorption efficiency

Source	Degree of freedom	Sum of squares	Mean square	$F_{statistic}$	Prob. > F
Model	14	14088.200	1006.30	40.6887	<.0001*
Residual	16	395.706	24.73	-	-
Total	30	14483.906	-	-	-

$F_{statistic}$: experimental Fisher factor ;

* : significant to 0.1 % ($F_{0.001}(14.16) = 5.27$)

3.10.2. *Effect of variables on PS biosorption efficiency*

The interactions of the four parameters and their main effects are gathered in Table 8. Each coefficient is associated with the F -value and p -value. The Fisher-test is used to determine the significance and the importance of factors effects and interactions between the variables on the response studied. Moreover, the large amplitude of F -value corresponds to the small p -value [60].

Table 8. Estimated regression coefficients and corresponding F and P values for PS biosorption efficiency.

Model term	Estimation	Sum of squares	F _{Statistics}	Prob.>F	Significance
Constant	82.367143	-	-	<.0001	***
pH	-21.25542	10843.026	438.4270	<.0001	***
[PS]	-4.972917	593.518	23.9983	0.0002	***
m(FS)	2.5995833	162.188	6.5579	0.0209	*
T	-0.927083	20.628	0.8341	0.3747	NS
pH*[PS]	-0.446875	3.195	0.1292	0.7240	NS
pH*m(FS)	-2.841875	129.220	5.2249	0.0362	*
[PS]*m(FS)	2.790625	124.601	5.0381	0.0393	*
pH*T	-2.728125	119.083	4.8150	0.0433	*
[PS]*T	1.586875	40.291	1.6291	0.2200	NS
m(FS)*T	-2.885625	133.229	5.3870	0.0338	*
pH*pH	-7.380432	1557.632	62.9813	<.0001	***
[PS]*[PS]	-2.516682	181.116	7.3233	0.0156	*
m(FS)*m(FS)	-3.075432	270.467	10.9360	0.0045	**
T*T	-3.344182	319.802	12.9309	0.0024	**

***: significant to 0.1% ($F_{0.001}(1.16)=16.12$) ;

**: significant to 1.0% ($F_{0.01}(1.16)=8.53$) ;

*: significant to 5.0% ($F_{0.05}(1.16)=4.49$) ;

NS: not significant

As shown in Table 8, except the linear effect of T and the interactions $pH*[PS]$, and $[PS]*T$, all other terms have significative effect. Moreover, for a level of confidence

of 99.9% the linear effects of pH and $[PS]$ and the quadratic effect of pH are significant with a very low p -values. However, it can be seen from results in Table 8 that for level of confidence of 99% the quadratic effects of $m(FS)$ and T are significant with a low p -values (0.0045 and 0.0024 respectively). Although, the p -values of linear effect of $m(FS)$, the interactions $pH*m(FS)$, $[PS]*m(FS)$, $pH*T$, $m(FS)*T$ and the quadratic effect of $[PS]$ are less than 0.05, implying that all these terms are significant for a level of confidence of 95%.

3.10.3. The second-order model of PS biosorption on FS efficiency (%)

To define the response variations according to the factors that influence the result, a polynomial model (second-order model) was chosen:

$$\begin{aligned} \text{Efficiency \%} = & 82.367143 - 21.25542 \text{ pH} - 4.972917 [\text{PS}] + 2.5995833 \text{ m(FS)} - \\ & 0.927083 \text{ T} - 0.446875 \text{ pH} * [\text{PS}] - 2.841875 \text{ pH} * \text{m(FS)} + 2.790625 [\text{PS}] * \text{m(FS)} - \\ & 2.7281 \text{ pH} * \text{T} + 1.586875 [\text{PS}] * \text{T} - 2.885625 \text{ m(FS)} * \text{T} - 7.380432 \text{ pH} * \text{pH} - 2.516682 \\ & [\text{PS}] * [\text{PS}] - 3.075432 \text{ m(FS)} * \text{m(FS)} - 3.344182 \text{ T} * \text{T} \end{aligned}$$

The polynomial model only considers factors having p -value <0.05 . According to Table 8, the polynomial model was defined as follows:

$$\begin{aligned} \text{Efficiency \%} = & 82.367143 - 21.25542 \text{ pH} - 4.972917 [\text{PS}] + 2.5995833 \text{ m(FS)} - \\ & 2.841875 \text{ pH} * \text{m(FS)} + 2.790625 [\text{PS}] * \text{m(FS)} - 2.7281 \text{ pH} * \text{T} - 2.885625 \text{ m(FS)} * \text{T} - \\ & 7.380432 \text{ pH} * \text{pH} - 2.516682 [\text{PS}] * [\text{PS}] - 3.075432 \text{ m(FS)} * \text{m(FS)} - 3.344182 \text{ T} * \text{T} \end{aligned}$$

3.10.4. Graphical study of the factor effect

Fig. 9 describes the effect of four factors on the PS biosorption efficiency. At first, it is observed that the pH reflects a negative effect on the response. Besides, above a PS concentration of 35 mg L^{-1} the effect of this factor become negative. For the FS mass, the effect on the response is positive until a value of 260 mg. However, the temperature has a low effect on PS biosorption efficiency.

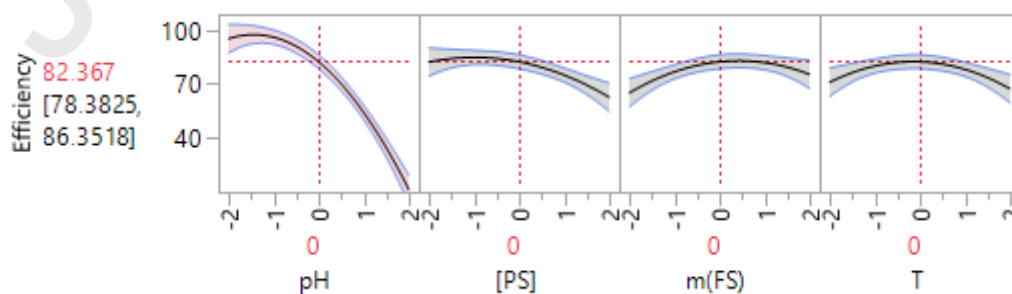


Fig. 9. Main effect plot of parameters on the PS biosorption efficiency

3.10.5. Validation of model

Fig. 10 gathers the correlation between experimental and predicted values, characterized by points clouds whose alignment is close to a straight line. The condition of normality of the residues is thus well respected for the model. Furthermore, the value of adjusted R^2 and R^2 , in this model, were evaluated as 0.9727 and 0.9488, respectively, indicating that only 5.12% of the variability in the response could not be defined by the model, for PS biosorption on FS efficiency.

Further, Fig. 10 reveals the experimental response values agree with the predicted values, which shows that there are tendencies in the linear regression fit. The proposed model adequately explains the experimental studied range. These results show that there is a statistical agreement between experimental and predicted values.

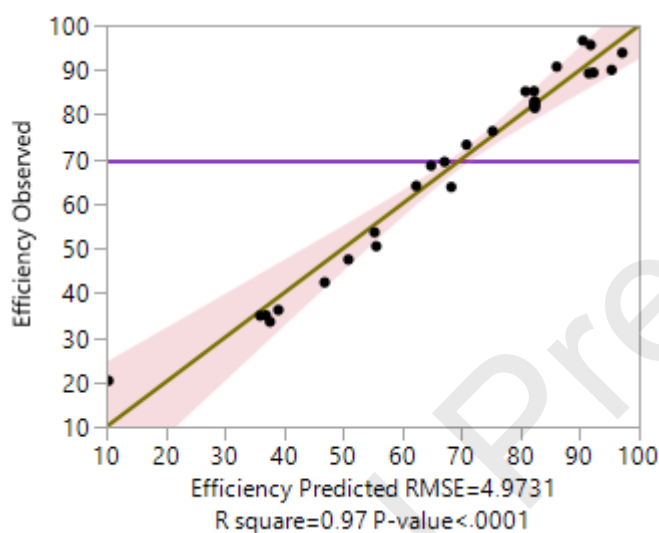


Fig. 10. Correlation between predicted and experimental values for PS biosorption on FS efficiency

3.10.6. Response surface plots and optimization conditions

Three-dimensional (3D) and contour (2D) plots for response surface were used to assess the relationships between the dependent response (PS biosorption on FS efficiency) and independent variables (pH and mass of FS) when PS concentration and temperature were kept constant at fixed values ($[PS] = 35 \text{ mg L}^{-1}$ and $T = 303 \text{ K}$). Results are presented in Fig. 11 showing that the mass increase of FS, and the decrease of pH, increased the PS biosorption efficiency.

The major objective of the optimization is the determination of the best values of variables for PS biosorption efficiency process from the model using experimental data. This result shows that the response surface presents a maximum point. Thereby, this

contour plot indicates an increase in PS biosorption in low pH at about 2.1-2.2, and high values of FS mass between 225 mg and 325 mg.

Therefore, working with these conditions ($[PS] = 35 \text{ mg L}^{-1}$; $T = 303 \text{ K}$; $\text{pH} = 2.1$; $m(\text{FS}) = 250 \text{ mg}$) the PS biosorption efficiency can reach a value higher than 96.58%.

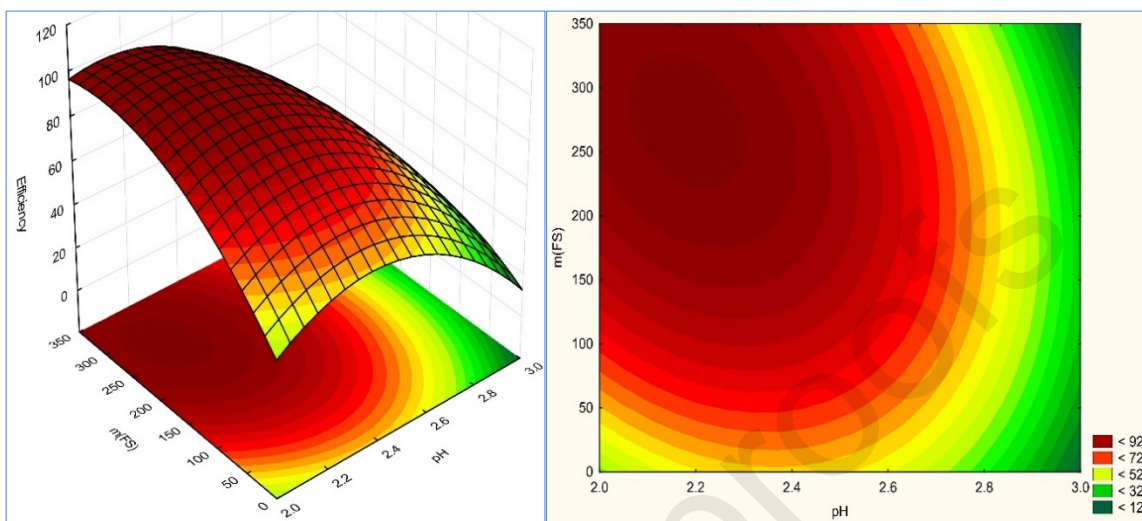


Fig. 11. Surface and contour plots of estimated response surface of PS biosorption efficiency

3.10.7. Comparison of PS biosorbents

A comparative study of the biosorption capacity for PS was carried out with other biosorbents (Table 9). It is obvious that FS shows a well efficiency comparing to Poly-vinyl alcohol enhanced hybrid hydrogels of hyper branched poly-(etheramine), Chitin, or nanosized niobium pentoxide (Nb_2O_5) with 4.256 mg g^{-1} , 5.2 mg g^{-1} or 41.0 mg g^{-1} , respectively. FS is also a better biosorbent than alumino-phosphate [21]. So, it is interesting that FS arising from a marine waste is a good and low-cost biosorbent and it could be investigated in the removal of another dyes.

Table 9. Comparison of maximum biosorption capacity of FS for PS with other adsorbents

Biosorbent	q_m (mg g^{-1})	Reference
Nanosized semiconductor Nb_2O_5	41.00	[7]
Chitin	5.20	[20]
AlPO_4	47.90	[21]
SDBS modified AlPO_4	60.81	[22]

PVA@SiO1.5	4.25	[60]
hPEA-1/2Gel		
Fish scale	56.50	<i>This work</i>

3.11. MC and RDF simulations

The MC calculation was used to predicting both behavior and strength biosorption of PS onto collagen and HDA surfaces. Before this analysis, it is also possible to obtain the radial distribution function (RDF) (or pair correlation function $G(R)$). The RDF is used as a technique to predict the nature of biosorption between PS and surface. The appearance of peaks from 1.00 Å to 3.50 Å is a sign of chemisorption interaction nature [31]. The stable biosorption configuration of the studied interfaces (PS/100water/50H₃O⁺/50Cl⁻/Collagen or HDA) (Fig. 12) and RDF plots are exposed in Fig. 13. To evaluate the biosorption between PS and collagen/or HDA such energies are calculated: the total energy (E_T) reports the global energy for the systems under study (PS/100water/50H₃O⁺/50Cl⁻/Collagen or HDA), this parameter is calculated by optimizing the whole system. Therefore, the biosorption energy (E_{ads}) which displays the energy required when the relaxed PS is adsorbed on the surface, this parameter is commonly recognized to estimate the strength and mechanism of biosorption. Then, the energy dE_{ads}/dN_i , namely the desorption energy, reports the necessary energy where one molecule PS removed to the system of (PS/100water/50H₃O⁺/50Cl⁻/Collagen or HDA).

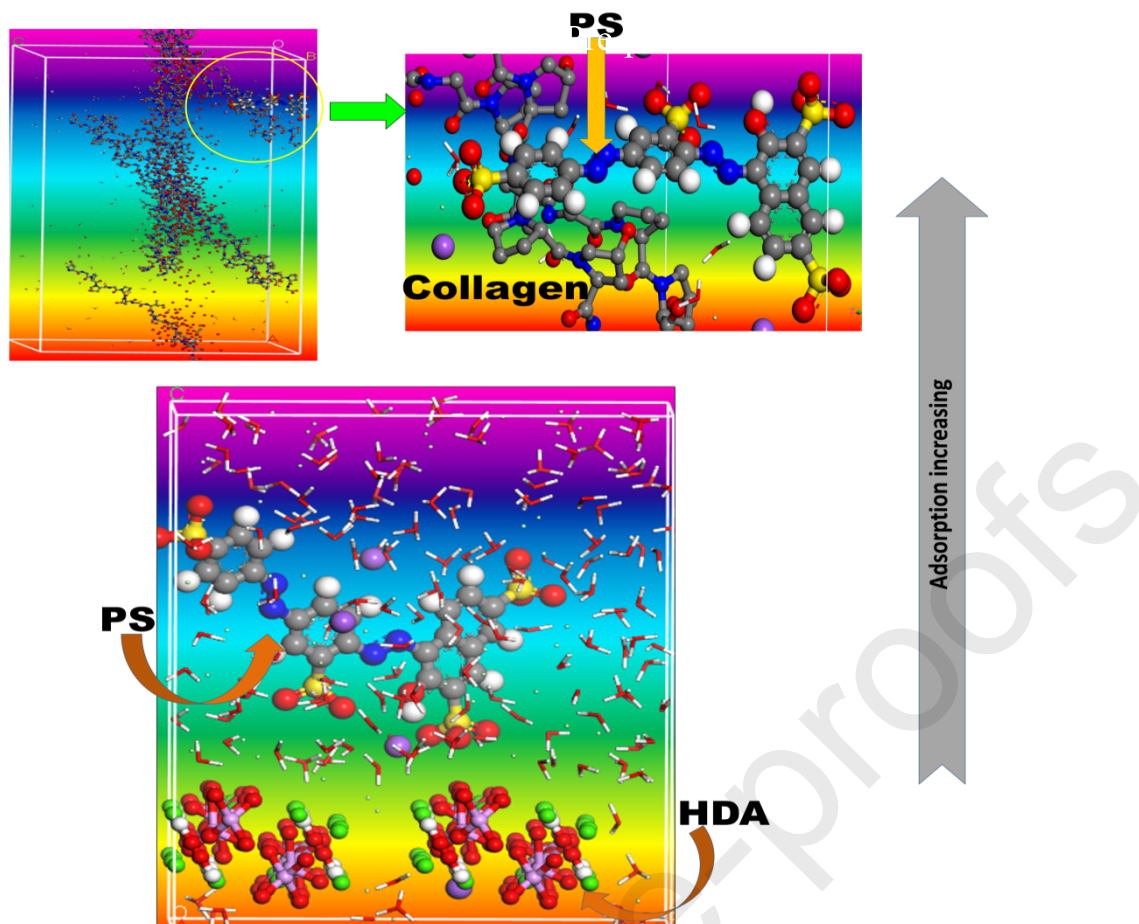


Fig. 12. Most stable configurations of two interfaces: PS/100water/50H₃O⁺/50Cl⁻/Collagen and PS/100water/50H₃O⁺/50Cl⁻/HDA at temperature of 297.15 K.

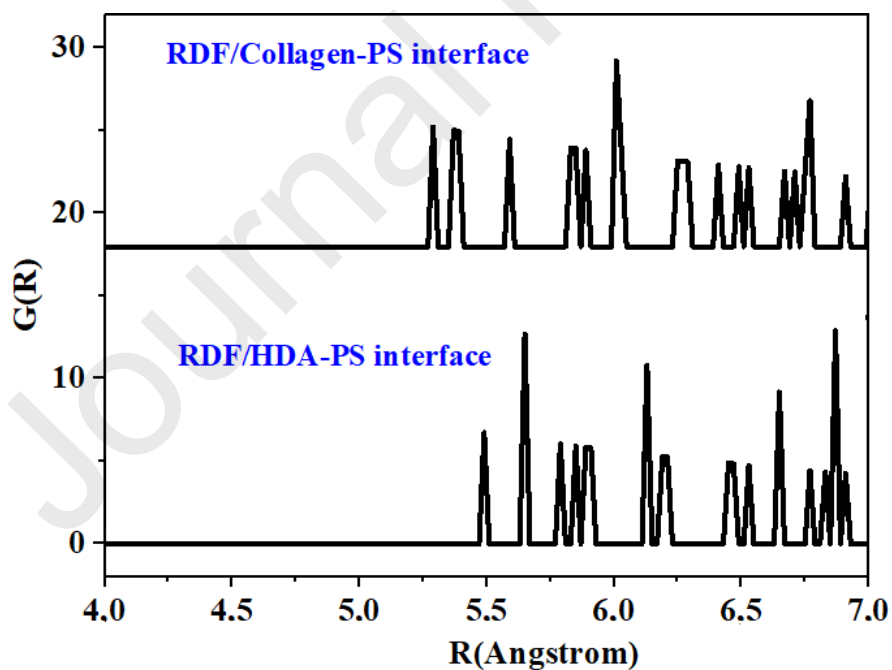


Fig. 13. RDF analysis of PS/100water/50H₃O⁺/50Cl⁻/Collagen or HDA interface

Table 10 shows that interface of PS/100water/50H₃O⁺/50Cl⁻/Collagen is more stable (Low value of $\epsilon_{\text{Tot}} = -281.319 \text{ kcal mol}^{-1}$) comparing to the PS/100water/50H₃O⁺/50Cl⁻/HDA one (high value of $\epsilon_{\text{Tot}} = -202.969 \text{ kcal mol}^{-1}$). In addition, the negative values of E_{ads} mean that the studied biosorption can be spontaneously shaped [31,61]. Moreover, we observed that the system of PS/100water/50H₃O⁺/50Cl⁻/Collagen has a more negative value of ϵ_{ads} ($-94.255 \text{ kcal mol}^{-1}$) comparing to the PS/100water/50H₃O⁺/50Cl⁻/HDA interface ($-14.631 \text{ kcal mol}^{-1}$); indicating a stronger interaction between PS and collagen surface. Furthermore, we perceived that $d\epsilon_{\text{ad}}/dN_i$ for PS molecule onto collagen surface is higher ($d\epsilon_{\text{ads}}/dN_i = -234.990 \text{ kcal mol}^{-1}$) than that onto HDA surface ($d\epsilon_{\text{ads}}/dN_i = -395.103 \text{ kcal mol}^{-1}$). This observation clearly shows that it is more difficult to detach a PS molecule from the collagen surface than from the HDA surface. For the RDF analysis (Fig. 13) the intense peaks correspond to the PS/100water/50H₃O⁺/50Cl⁻/Collagen or HDA interface seems at the link lengths greater than 3.50 Å. This result reveals that the adsorption process is a physisorption one.

Table 10. Outputs and descriptors calculated by the MC simulation for biosorption of PS on the collagen or HDA surface (in kcal mol⁻¹).

	ϵ_{Tot}	ϵ_{Ads}	$d \epsilon_{\text{Ads}}/dN_i$ (PS)
PS/collagen	-281.319	-94.255	-234.990
PS/HDA	-202.969	-14.631	-395.103

4. Conclusion

FS has been investigated as a biosorbent to uptake PS dye from aqueous solutions. The results showed an excellent removal capacity and gave a good biosorption efficiency. At the optimized conditions (e.g. FS mass of 250 mg; contact time of 60 min; PS concentration of 35 mg L⁻¹; V = 200 mL; pH = 2.10; temperature = 296 K), 96.58% of PS dye were removed. Under the same optimized conditions, the maximum biosorption capacity for PS dye was identified to be 56.50 mg g⁻¹. In addition, PS dye was desorbed in alkaline pH. These results were confirmed with a CCD according to the RSM, the results of optimization showed that at a pH of 2.1, and a concentration of PS of 35 mg L⁻¹, and weight of FS of 250 mg and a temperature of 303 K, the biosorption reached more than 96% of treatment efficiency.

The biosorption phenomenon of PS by FS is favorably influenced by a temperature decrease. The biosorption kinetics followed the pseudo-first-order expression. The process was thermodynamically spontaneous. In addition, the feasibility of the

biosorption was confirmed by a good fitting with Freundlich isotherm model. Finally, the biosorption mechanism of two studied interfaces is highlighted using Monte Carlo and radial distribution function simulations.

Acknowledgments

The authors would like to thank the ESEF of Berrechid at Hassan First University (Morocco) and the ENSC of Rennes, CNRS and the Institute of Chemical Sciences of Rennes (France).

Conflict of interest

The authors declare that they have no conflict of interest.

References

- [1] Shah, MP, Patel, KA, Nair, SS, Darji, AM, 2013. Microbial degradation of textile dye (Remazol Black B) by *Bacillus* spp. ETL-2012. *J. Bioremed. Biodeg.* **4**, 1-5.
- [2] Robinson, T, Mullan, GM, Marchant, R, Nigam, P, 2001. Remediation of dyes in textile effluent: a critical review on current treatment technologies with a proposed alternative. *Bioresour. Technol.* **77**, 247-255.
- [3] Pearce, CI, Lloyd, JR, Guthrie, JT, 2003. The removal of colour from textile wastewater using whole bacterial cells: a review. *Dyes and Pigments* **58**, 179-196.
- [4] Bannur, SV, Kulgod, SV, Metkar, SS, Mahajan, SK, Sainis, JK, 1999. Protein determination by Ponceau S using digital color image analysis of protein spots on nitrocellulose membranes. *Analyt. Biochem.* **267**, 382–389.
- [5] Meena, RC, Pachwarya, RB, Meena, VK, Arya, S, 2009. Degradation of textile dyes Ponceau-S and Sudan IV using recently developed photocatalyst, immobilized resin Dowex-11. *Am. J. Environ. Sci.* **5**, 444–450.
- [6] Venkatesha, TG, Nayaka, YA, Chethana, BK, 2013. Adsorption of Ponceau S from aqueous solution by MgO nanoparticles. *Appl. Surf. Sci.* **276**, 620-627.
- [7] Patil, BN, Naik, DB, Shrivastava, VS, 2011. Photocatalytic degradation of hazardous Ponceau-S dye from industrial wastewater using nanosized niobium pentoxide with carbon. *Desalination* **269**, 276-283.
- [8] Pachwarya, RB, Meena, RC, 2011. Degradation of azo dyes Ponceau S, S-IV from the wastewater of textile industries in a new photocatalytic reactor with high efficiency using recently developed photocatalyst MBIRD-11. *Energy Sources, Part A: Recovery, Utilization Environ. Eff.* **33**, 1651-1660.

- [9] Marathe, SD, Shrivastava, VS, 2014. Synthesis, characterization and photocatalytic application of nanosized PbO in the removal of hazardous Ponceau S dye in the presence of UV light. *Advanced Sci. Focus* **2**, 8-11.
- [10] Hossain, MM, Hossain, MA, Kayes, MN, Halder, D, 2014. ZnO mediated photodegradation of aqueous solutions of crystal violet and Ponceau S by visible light. *J. Eng. Sci.* **5**, 69-74.
- [11] Muslim, M, Habib, MA, Mahmood, AJ, Islam, TSA, Ismail, IMI, 2012. Zinc oxide-mediated photocatalytic decolorization of Ponceau S in aqueous suspension by visible light. *International Nano Lett.* **2**,. <https://doi.org/10.1186/2228-5326-2-30>
- [12] Marathe, SD, Shrivastava, VS, 2015a. Removal of hazardous Ponceau S dye from industrial wastewater using nano-sized ZnO. *Desalination Water Treatment* **54**, 2036-2040.
- [13] Marathe, SD, Shrivastava, VS, 2015b. Photocatalytic removal of hazardous Ponceau S dye using nanostructured Ni-doped TiO₂ thin film prepared by chemical method. *Appl. Nanosci.* **5**, 229-234.
- [14] Sahoo, MK, Marbaniang, M, Sinha, B, Naik, DB, Sharan, RN, 2012. UVC induced TOC removal studies of Ponceau S in the presence of oxidants: Evaluation of electrical energy efficiency and assessment of biotoxicity of the treated solutions by *Escherichia coli* colony forming unit assay. *Chem. Eng. J.* **213**, 142-149.
- [15] Sahoo, MK, Marbaniang, M, Sharan, RN, 2016. UV light-assisted mineralization and biodegradation of Ponceau S with hydroxyl and sulfate radicals. *Chemical Papers.* **70**, 1066–1077.
- [16] Muslim, M, Habib, MA, Islam, TSA, Ismail, IMI, Mahmood, AJ, 2013. Decolorization of diazo dye Ponceau S by Fenton process. *Pak. J. Anal. Environ. Chem.* **14**, 44-50.
- [17] Sahoo, MK, Marbaniang, M, Sinha, B, Sharan, RN, 2014. Fenton and Fenton-like processes for the mineralization of Ponceau S in aqueous solution: Assessment of ecotoxicological effect of post treated solutions. *Sep. Purif. Technol.* **124**, 155-162.
- [18] El Desoky, HS, Ghoneim, MM, Zidan, NM, 2010. Decolorization and degradation of Ponceau S azo-dye in aqueous solutions by the electrochemical advanced Fenton oxidation. *Desalination* **264**, 143-150.
- [19] Li, G, Zhu, Z, Qi, B, Liu, G, Wu, P, Zeng, G, Zhang, Y, Wang, W, Sun, Y, 2016. Rapid capture of Ponceau S via hierarchical organic-inorganic hybrid nanofibrous membrane. *J. Mater. Chem. A* **4**, 5423-5427.

- [20] Shirsath, DS, Shrivastava, VS, 2012. Removal of hazardous dye Ponceau-S by using chitin: An organic biosorbent. *African J. Environ. Sci. Technol.* **6**, 115-124.
- [21] Flilissa, A, Sebaihi, W, Sivasankar, V, Boutahala, M, Darchen, A, 2017. Removal of Ponceau S by adsorption onto alumino-phosphate. *Desalination Water Treatment* **60**, 170–179.
- [22] Flilissa, A, Venkataraman, S, Laouameur, K, Beroual, A, Flilissa, O, Omine, K, Chaabane, T, Darchen, A, 2020. Surface modification of aluminum phosphate by sodium dodecylbenzenesulfonate (SDBS): A new nano-structured adsorbent for an improved removal of Ponceau S. *J. Environ. Chem. Eng.* **8**, 103625, <https://doi.org/10.1016/j.jece.2019.103625>
- [23] Ighalo, JO, Eletta, OAA, 2020. Recent advances in the biosorption of pollutants by fish scales: a mini-review. *Chemical Engineering Communications*, <https://doi.org/10.1080/00986445.2020.1771322>
- [24] Eletta, OAA, Ighalo, JO, 2019. A review of fish scales as a source of biosorbent for the removal of pollutants from industrial effluents. *J. Res. Information Civil Eng.* **16**, 2479- 2510.
- [25] Fabiano, CR, Scheufele, B, Espinoza-Quñones, FR, Módenes, AN, da Silva, MGC, Vieira, MGA, Borba, CE, 2015. Characterization of *Oreochromis niloticus* fish scales and assessment of their potential on the adsorption of reactive blue 5G dye. *Colloid Surf. A Physicochem. Eng. Asp.* **482**, 693-70.
- [26] Marrakchi, F, Ahmed, MJ, Khanday, WA, Asif, M, Hameed, BH, 2017. Mesoporous carbonaceous material from fish scales as low-cost adsorbent for reactive Orange 16 adsorption. *J. Taiwan Inst. Chem. Eng.* **71**, 47–54.
- [27] Jaafar, A, Driouich, A, Lakbaibi, Z, Ben El Ayouchia, H, Azzaoui, K, Boussaoud, A, Jodeh, S, 2019. Central composite design for the optimization of Basic Red V degradation in aqueous solution using Fenton reaction. *Desalination Water Treatment*. **158**, 364–371.
- [28] Tarhan, T, Tural, B, Boga, K, Tural, S, 2019, Adsorptive performance of magnetic nano-biosorbent for binary dyes and investigation of comparative biosorption. *SN Applied Sciences*, **1**, 1-11, <https://doi.org/10.1007/s42452-018-0011-1>
- [29] Tural, B, Ertaş, E, Enez, B, Fincan, SA, Tural, S, 2017. Preparation and characterization of a novel magnetic biosorbent functionalized with biomass of *Bacillus Subtilis*: Kinetic and isotherm studies of biosorption processes in the removal of Methylene Blue. *J. Environ. Chem. Eng.* **5**, 4795-4802.

- [30] Tural, S, Tarhan, T, Tural, B, 2016. Removal of hazardous azo dye Metanil Yellow from aqueous solution by cross-linked magnetic biosorbent; equilibrium and kinetic studies. *Desalination Water Treatment* **57**, 13347-13356.
- [31] Jaafar, A, Darchen, A, El Hamzi, S, Lakbaibi, Z, Driouich, A, Boussaoud, A, Yaacoubi, A, El Makhfouk, M, Hachkar, M, 2020. Optimization of cadmium ions biosorption by fish scale from aqueous solutions using factorial design analysis and Monte Carlo simulation studies. *J. Environ. Chem. Eng*, **9**, 104727, <https://doi.org/10.1016/j.jece.2020.104727>
- [32] Jodeh, S, Shawahny, M, Hanbali, G, Jodeh, D, Dagdag, O, 2021. Efficiency of magnetic chitosan supported on graphene for removal of perchlorate ions from wastewater. *Environ. Technol.* **42**, 1119-1131.
- [33] Ghaedi, M, Hajati, S, Barazesh, B, Karimi, F, Ghezelbash, G, 2013. *Saccharomyces cerevisiae* for the biosorption of basic dyes from binary component systems and the high order derivative spectrophotometric method for simultaneous analysis of Brilliant green and Methylene blue. *J. Indust. Eng. Chem.* **19**, 227-233.
- [34] Muntean, SG, Nistor, MA, Ianoş, R, Păcurariu, C, Căpraru, A, Surdu, VA, 2019. Combustion synthesis of Fe₃O₄/Ag/C nanocomposite and application for dyes removal from multicomponent systems. *Appl. Surf. Sci.* **481**, 825-837.
- [35] Vishan, I, Saha, B, Sivaprakasam, S, Kalamdhad, A, 2019. Evaluation of Cd(II) biosorption in aqueous solution by using lyophilized biomass of novel bacterial strain *Bacillus badius* AK: Biosorption kinetics, thermodynamics and mechanism. *Environ. Technol. Innova.* **19**, 100323. <https://doi.org/10.1016/j.eti.2019.100323>
- [36] Langmuir, I, 1918. The adsorption of gases on plane surfaces of glass, mica, and platinum. *J. Am. Chem. Soc.* **40**, 1361-1368.
- [37] Freundlich, HMF, 1906. Over the adsorption in solution. *J. Phys. Chem.* **57**, 385-470.
- [38] Gimbert, F, Morin-Crini, N, Renault, F, Badot, PM, Crini, G, 2008. Adsorption isotherm models for dye removal by cationized starch-based material in a single component. *J. Hazard. Mater.* **157**, 34-46.
- [39] Sykam, N, Jayram, ND, Rao, GM, 2019. Exfoliation of graphite as flexible SERS substrate with high dye adsorption capacity for Rhodamine 6G. *Appl. Surf. Sci.* **471**, 375-386.
- [40] Maleki, A, Hayati, B, Naghizadeh, M, Joo, SW, 2015. Adsorption of hexavalent chromium by metal organic frameworks from aqueous solution. *J. Ind. Eng. Chem.* **28**, 211-216.

- [41] Zheng, Y, Liu, J, Cheng, B, You, W, Ho, W, Tang, H, 2019. Hierarchical porous Al₂O₃@ZnO core-shell microfibres with excellent adsorption affinity for Congo red molecule. *Appl. Surf. Sci.* **473**, 251-260.
- [42] Yu, S, Wang, X, Pang, H, Zhang, R, Song, W, Fu, D, Hayat, T, Wang, X, 2018. Boron nitride-based materials for the removal of pollutants from aqueous solutions: a review. *Chem. Eng. J.* **333**, 343-360.
- [43] WeiB, CH, 2007. StatSoft, Inc., Tulsa, OK.: STATISTICA, version 8. AStA *Advances in Statistical Analysis*, **91**, 339-341.
- [44] SAS Institute Inc, JMP 10 Basic Analysis and Graphing, Second Edition USA, (2012).
- [45] Sun, H, 2006. COMPASS: an ab initio force-field optimized for condensed-phase applications overview with details on alkane and benzene effect of triphenyltin 2-thiophene carboxylate on corrosion of steel in 2 M H₃PO₄ solutions. *Appl. Surf. Sci.* **252**, 8341-8347.
- [46] Regti, A, Lakbaibi, Z, Ben Elayouchia, H, El Haddad, M, Laamari, MR, Jaafar, A, Elazhary, I, El Himri, M, 2021. Optimization and computational approach to understand the adsorption behavior of Alizarine Red S on the surface of fish scales. *Biointerface Research in Applied Chemistry*, **11**, 14918-14934.
- [47] Kara, A, Tamburaci, S, Tihminlioglu, F, Havitcioglu, H, 2019. Bioactive fish scale incorporated chitosan biocomposite scaffolds for bone tissue engineering. *Int. J. Biol. Macromol.* **130**, 266-279.
- [48] Ikoma, T, Kobayashi, H, Tanaka, J, Walsh, D, Mann, S, 2003. Microstructure, mechanical, and biomimetic properties of fish scales from *Pagrus major*. *J. Struct. Biol.* **142**, 327-333.
- [49] Bose, S, Saha, SK, 2003. Synthesis and characterization of hydroxyapatite nanopowders by emulsion technique. *Chem. Mater.* **15**, 4464-4469.
- [50] Paul, S, Pal, A, Choudhury, AR, Bodhak, S, Balla, VK, Sinha, A, Das, M, 2017. Effect of trace elements on the sintering effect of fish scale derived hydroxyapatite and its bioactivity. *Ceram. Int.* **43**, 15678-15684.
- [51] Zainol, I, Adenan, NH, Rahim, NA, Jaafar, CAN, 2019. Extraction of natural hydroxyapatite from tilapia fish scales using alkaline treatment. *Mater. Today: Proc.* **16**, 1942-1948.
- [52] Das, B, Mondal, NK, 2011. Calcareous soil as a new adsorbent to remove lead from aqueous solution: equilibrium, kinetic and thermodynamic study. *Universal J. Environ. Res. Technol.* **1**, 515-530.

- [53] Lewinsky, AA (Editor), 2007. Hazardous materials and wastewater: treatment, removal and analysis. *Nova Science*, New York.
- [54] Tran, HN, You, SJ, Chao, HP, 2016. Thermodynamic parameters of cadmium adsorption onto orange peel calculated from various methods: A comparison study. *J. Environ. Chem. Eng.* **4**, 2671–2682.
- [55] Tran, HN, You, SJ, Hosseini-Bandegharai, A, Chao, HP, 2017. Mistakes and inconsistencies regarding adsorption of contaminants from aqueous solutions: a critical review. *Water Res.* **120**, 88–116.
- [56] Zhou, X, Zhou, X, 2014. The unit problem in the thermodynamic calculation of adsorption using the Langmuir equation, *Chem. Eng. Commun.* **201**, 1459–1467.
- [57] Papita, S, Shamik, C, 2011. Insight into adsorption thermodynamics, *Thermodynamic*, INTECH Open Access Publisher, 349–364.
- [58] Kankılıç, GB, Metin, AU, Tüzün, I, 2016. *Phragmites australis*: An alternative biosorbent for basic dye removal. *Ecological Eng.* **86**, 85-94.
- [59] Dallel, R, Kesraoui, A, Seffen, M, 2018. Biosorption of cationic dye onto *Phragmites australis* fibers: characterization and mechanism. *J. Environ. Chem. Eng.* **6**, 7247-7256.
- [60] Deng, S, Xu, H, Jiang, X, Yin, J, 2013. Poly-vinyl alcohol (PVA)-enhanced hybrid hydrogels of hyper branched poly (etheramine) (hPEA) for selective adsorption and separation of dyes. *Macromolecules* **46**, 2399–2406.
- [61] Chebabe, D, About, S, Damej, M, Oubair, A, Lakbaibi, Z, Dermaj, A, Benassaoui, H, Doubi, M, Hajjaji, N, 2020. Electrochemical and theoretical study of corrosion inhibition on carbon steel in 1M HCl medium by 1,10-bis(4-amino-3-methyl-1,2,4-triazole-5-thioyl)decane. *J. Fail. Anal. and Preven.* **20**, 1673–1683.

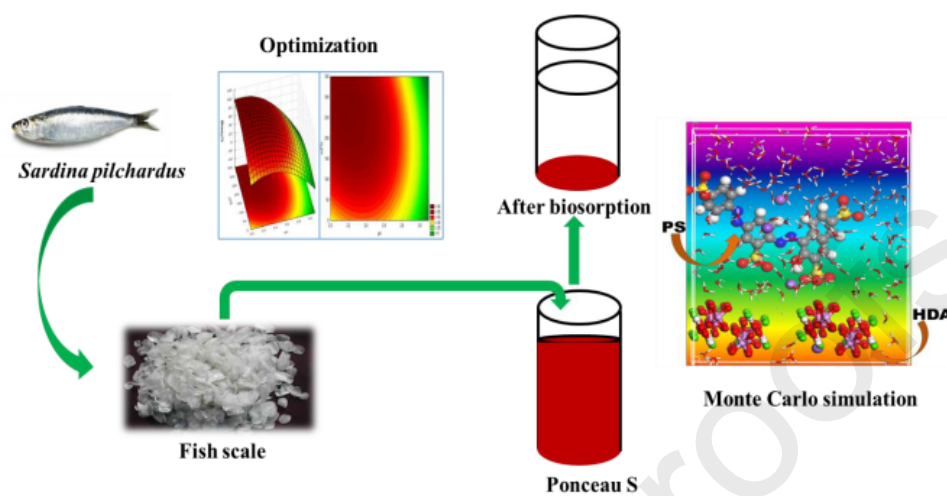
Author statement

Fish scale of *Sardina pilchardus* as a biosorbent for the removal of Ponceau S dye from water: Experimental, designing and Monte Carlo investigations

Manuscript N° INOCHE-D-21-00944

Adil Jaafar: Conceptualization, Investigation, Methodology, Software, Writing - Original Draft, Resources, Writing - Review & Editing, Visualization. **André Darchen:** Conceptualization, Investigation, Methodology, Methodology, Writing - Original Draft, Writing - Review & Editing. **Anas Driouich:** Methodology, Software, Visualization. **Zouhair Lakbaibi:** Conceptualization, Methodology, Software. **Abdelghani Boussaoud:** Conceptualization, Investigation, Resources. Supervision. **Baylassane Chatib:** Resources. **Yasmine Laftani:** Resources. **El Makhfouk Mohammed:** Resources. **Mohsine Hachkar:** Resources.

Graphical abstract



Highlights

- Fish scales were investigated as biosorbent in the removal of Ponceau S (PS) dye
- The parameters were optimized by using a Central Composite Design methodology
- With optimized conditions the PS removal reached an efficiency greater than 96%
- Pseudo-first order kinetics and Freundlich isotherm model gave the best fit
- The biosorption of PS onto fish scales was studied by a Monte Carlo investigation

Journal Pre-proofs

Declaration of interests

The authors declare that they have no known competing financial interests or personal relationships that could have appeared to influence the work reported in this paper.

The authors declare the following financial interests/personal relationships which may be considered as potential competing interests:

Journal Pre-proofs